

MEASUREMENTS OF DYNAMIC FRICTION CHARACTERISTICS OF THE BELT-PULLEY CONTACT UNDER DRY CONDITIONS

KRZYSZTOF KUBAS¹

Abstract

The paper presents the results of measurements of friction forces achieved by forcing slip between a poly-V 5pk belt and the pulley needed to formulate empirical models of dynamic friction. This kind of belt and pulley can be found in automotive industry to drive the alternator and coolant pump in cars. The forces were measured for several cases of assumed preload and two cases of wrap angle. The complicated stick and slip processes are simplified by assuming an average effective dynamic friction coefficient. The results show that the values of friction cannot be described by classic Euler formula. They not only depend on the velocity, but also noticed that can depend on sign of acceleration. Also, some results of the approximation are presented. It is proposed that the assumed norm will be minimised using the Nelder-Mead optimisation method. The measurements and the approximation let assume specified dynamic friction characteristics. The achieved results are applied to the model of a belt transmission. In the paper presented results of simulations of the model of belt transmission.

Keywords: belt-and-pulley transmission; dry friction; dynamic friction characteristics

1. Introduction

Many studies describe measurements of the belt friction forces. Works presenting results of investigations about belts conducted in centuries up to 1981 were summarised in a widely cited article [7].

Especially interesting are works presented, among others, in [3, 13], where some nonlinear models of dynamic friction coefficient were proposed. However, in that cited study, the Authors loaded the belt with a preload force of only up to 411 N. In this paper, results with a larger scale of friction preload are presented.

The experimental studies of contaminated by oils [6, 12, 15], water [6, 12, 16] or ice [5], water detergent [6] or aged belts [5] are also worth mentioning.

The results of the experiments help to create new friction models between the belt and the pulleys or to fit values of coefficients to existing ones. The Elastic/Perfectly Plastic (EPP) friction model [8] and Creep-Rate-Dependent Friction Law [10, 11] are examples of more complicated models of friction.

¹ Department of Mechanics, Faculty of Mechanical Engineering and Computer Science, University of Bielsko-Biala, ul. Willowa 2, 43-309 Bielsko-Biala, Poland, e-mail: kkubas@ath.bielsko.pl

The dynamic friction coefficient in the belt-pulley contact is difficult to measure because of the flexibility of rubber. When slip occurs, there are two possible situations: only a part of the belt contacting the pulley moves over the pulley and the rest of it does not slip (but it can deflect because of its flexibility) or, when slip is relatively large, all contacting parts of the belt slip on the pulley. The existing slip and non-slip regions were described, among others, in [1, 8, 11]. Transmission power losses caused by, among others, specified wrap angles or belt tension, have been described in [14].

It decided to measure poly-V 5pk belt with corresponding pulley. This kind of belt can be found, among others, in automotive industry to drive the alternator and coolant pump. Wrong or old contaminated rubber may change friction coefficients, what can cause noises, or their improper work of the transmission. This may cause the battery to fail or the engine to over-heat. It is therefore very important to measure frictional parameters of the belt and the pulley.

2. Measurements

It decided to simplify the measurements to some average values of the effective friction coefficient calculated directly from frictional forces, without considering them as force components in belt grooves. Such an assumption would correspond to the situation in which the friction in the flat belt is measured but generating the same frictional forces as in the case of a multi-groove belt. This assumption seems to be sufficient when results are needed in order to develop an empirical model of friction. The dependence between the effective friction coefficient μ and the real dynamic friction coefficient μ_D can be calculated from the friction force product in groove. It can be described by the following formula:

$$\mu_D = \mu \sin\left(\frac{\beta}{2}\right), \quad (1)$$

where:

$\beta=40^\circ$ – groove angle of the analysed poly-V belt.

In the Figure 1 shown the research stand that allowed to measure friction parameters in a belt transmission, especially between the belt and the pulley.



Fig. 1. Research stand for measuring friction parameters of a belt transmission

In the Figure 2 shown the scheme of measuring process. As can be seen from the figure, the presented stand allows setting a preload force of the belt F_0 and a wrap angle α . Preload force can be changed by tensioning screw. Wrap angle can be regulated by changing mounting point of one end of the belt. Load torque M_l can be applied by the AC motor, by manually changing the input values of the inverter. The irregularity of the set of values allows achieving more complex readings for different values of angular velocities and accelerations of the pulley, which would be difficult to achieve by automatically changing the input. Tensioning forces F_1 and F_2 of the belt can be measured by two force sensors applied to its ends.

The unsteady conditions allow measuring the so-called dynamic characteristics of the dynamic friction coefficient. It is worth mentioning that there are also the so-called kinetic characteristics of dynamic friction, which are achieved under steady conditions of velocity.

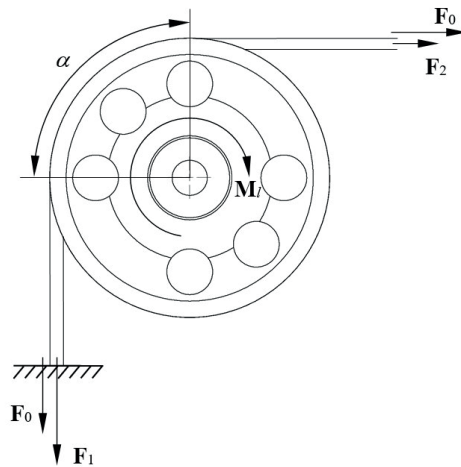


Fig. 2. Load torque M_l , friction preload F_0 and resulting forces F_1 and F_2 during measurements on the research stand

When there is no torque applied to the pulley, axial forces on both ends of the belt have the same value $F_1 = F_2 = F_0$. When the torque M_l is applied to the pulley, with the direction shown in the figure (in the clockwise direction), the lower force F_1 increases and the upper force F_2 simultaneously decreases to some boundary values. At this moment, the pulley starts to slip with some angular velocity ω . The main purpose was to measure changes of these forces during forcing belt slip.

The study assumed two cases of wrap angle $\alpha = 45^\circ$ and 90° , and an angular velocity in one – clockwise (assumed as positive) direction. It was also assumed according to the following values of the preload force F_0 : 200 N, 300 N, 400 N, 500 N, 600 N, 700 N, 800 N, 900 N and 1000 N.

In the Figure 3 and Figure 4 shown the measured values of F_1 (series of upper values) and F_2 (series of lower values) for the assumed values of preload force F_0 , as a function of angular velocity ω , for wrap angles $\alpha = 45^\circ$ and 90° , respectively.

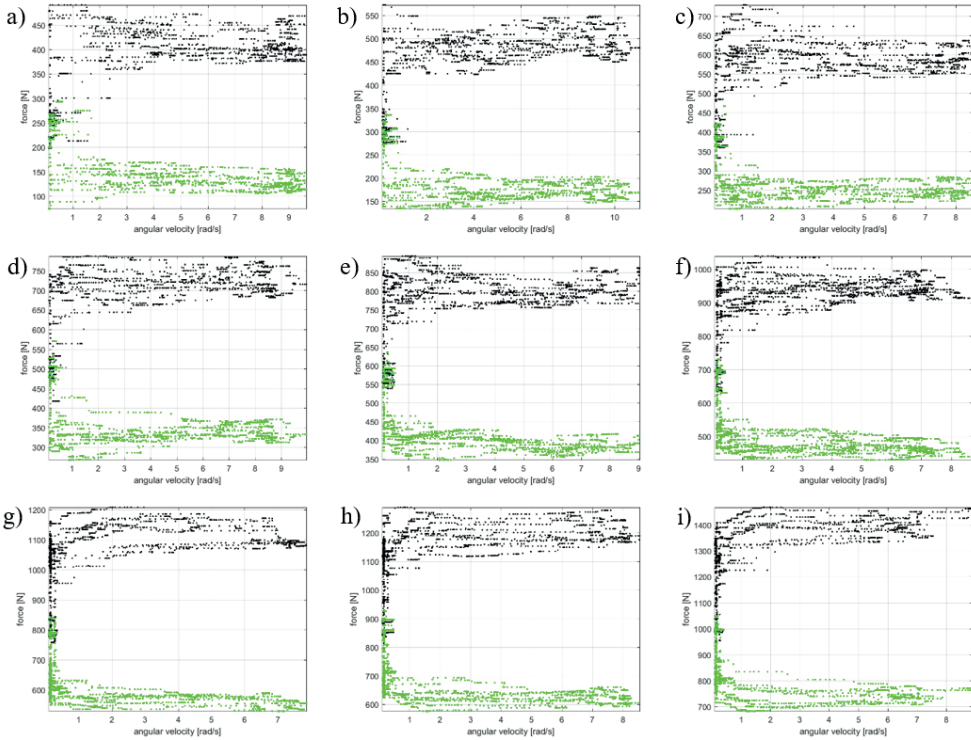


Fig. 3. Measured values of F_1 and F_2 as a function of angular velocity ω , for assumed values of wrap angle $\alpha = 45^\circ$ and preload force F_0 :
 a) 200 N, b) 300 N, c) 400 N, d) 500 N, e) 600 N, f) 700 N, g) 800 N, h) 900 N, i) 1000 N

• values of F_1 , • values of F_2

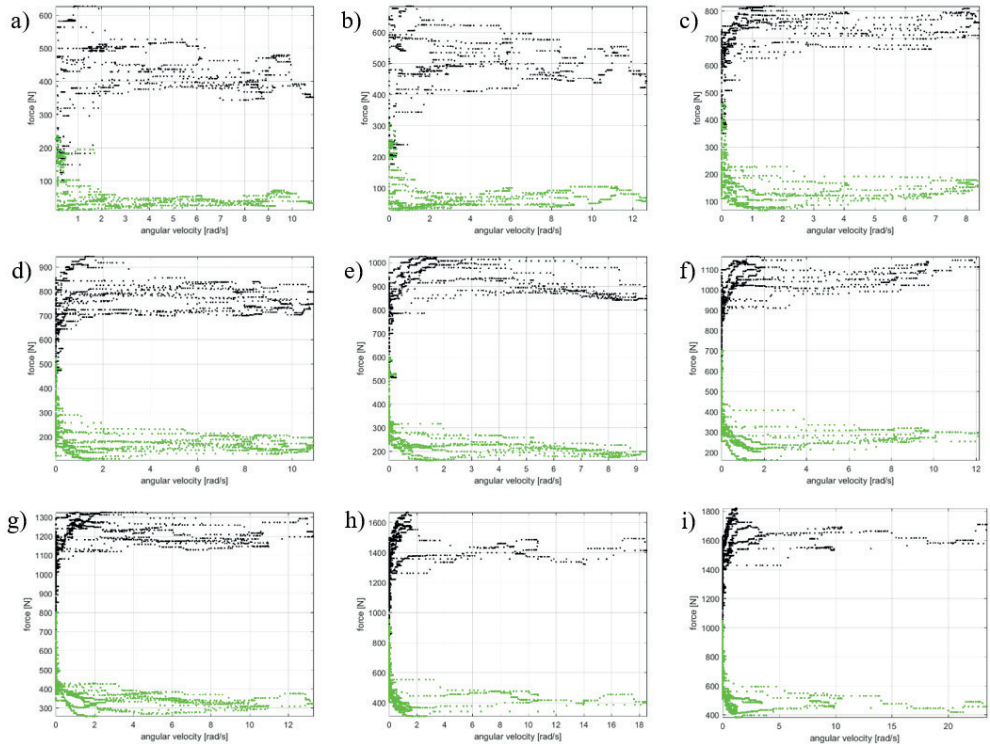


Fig. 4. Measured values of F_1 and F_2 as a function of angular velocity ω , for assumed values of wrap angle $\alpha = 90^\circ$ and preload force F_0 :
a) 200 N, b) 300 N, c) 400 N, d) 500 N, e) 600 N, f) 700 N, g) 800 N, h) 900 N, i) 1000 N

• values of F_1 , • values of F_2

As can be seen from the figures, generally, differences between values F_1 and F_2 of forces increase with increasing preload force F_0 . It can also be noticed that the change of the wrap angle α from 45° to 90° also causes an increase of these values.

Using the well-known Euler-Eytelwein formula:

$$\frac{F_1}{F_2} = e^{\mu\alpha}, \quad (2)$$

some average values of the effective dynamic friction coefficient along the entire wrap angle as a function of translational velocity in slip joint were calculated. The velocity was recalculated to translational velocity using a simple formula:

$$v = \omega \cdot r, \quad (3)$$

where:

$r = 0.06$ m – radius of the pulley.

The values of the effective dynamic friction coefficient for all values of friction preload, for wrap angle $\alpha = 45^\circ$ shown in the Figure 5 and in the Figure 6, and also for wrap angle $\alpha = 90^\circ$.

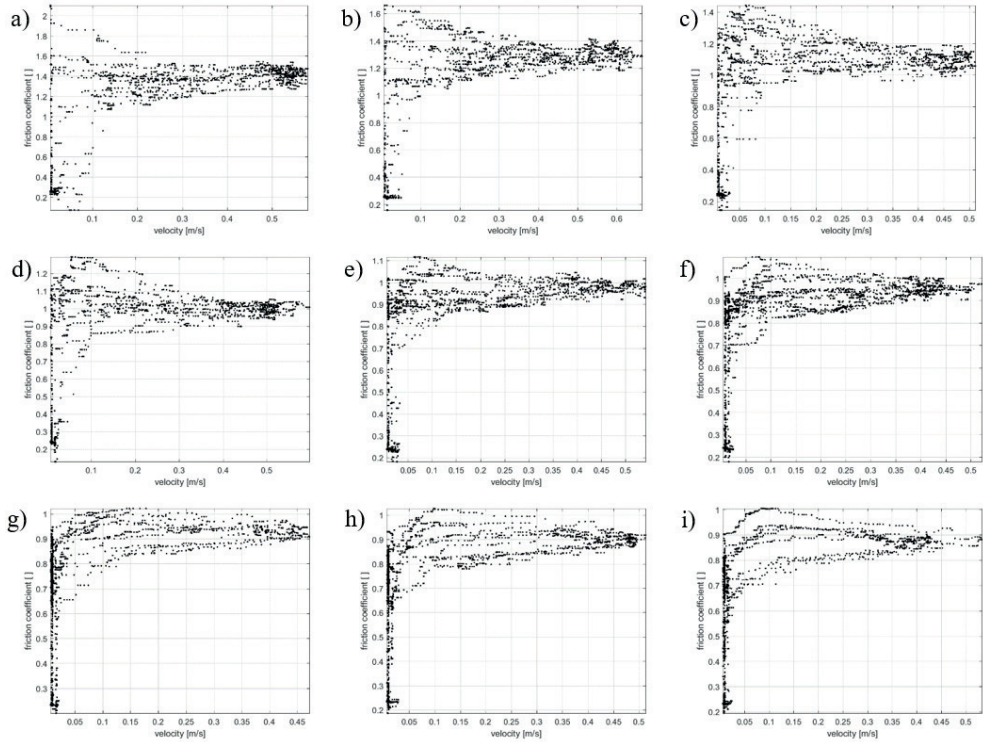


Fig. 5. Calculated values of effective dynamic friction coefficients as a function of translational velocity for wrap angle $\alpha = 45^\circ$ and preload force F_G :
 a) 200 N, b) 300 N, c) 400 N, d) 500 N, e) 600 N, f) 700 N, g) 800 N, h) 900 N, i) 1000 N

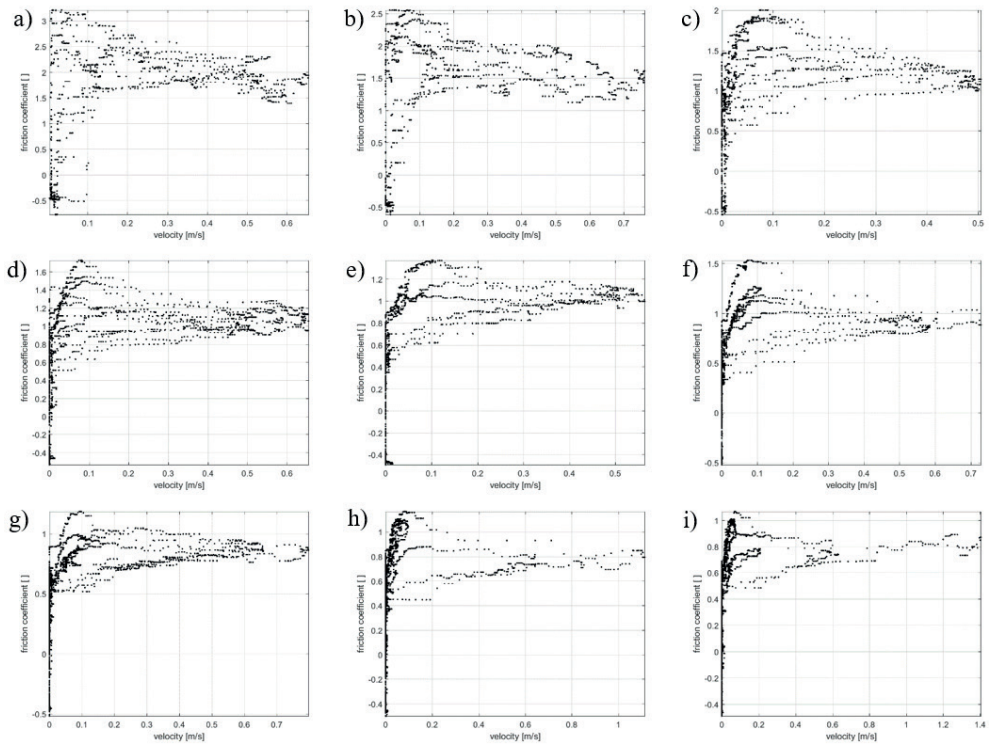


Fig. 6. Calculated values of effective dynamic friction coefficients as a function of translational velocity for wrap angle $\alpha = 90^\circ$ and preload force F_0 :
 a) 200 N, b) 300 N, c) 400 N, d) 500 N, e) 600 N, f) 700 N, g) 800 N, h) 900 N, i) 1000 N

As can be noticed, it is difficult to estimate the values of the dynamic friction coefficient for small values of velocity. As mentioned before, one of the reasons for this is the difficulty of predicting the size of the part of the sticking belt and how large the part moving over the pulley is. Another reason is the elasticity of the rubber. For larger values of the velocity, the calculated values of the dynamic friction coefficient are more possible to estimate.

It can also be seen from the Figure 5 and Figure 6 that when the preload force increases, the values of the friction coefficient simultaneously decreases. It is possible that after increasing normal forces, the structure of the surface changes with weaker frictional properties (maybe because, under pressure, the surface becomes flatter). This is also a proof that the classic Euler-Eytelwein formula is not appropriate for describing friction in those cases.

It is worth mentioning that the maximal values of the assumed preload forces are much greater than those permissible by manufacturers. The measured values of friction coefficients should, therefore, be treated as critical ones and, for example, they can correspond with some unusual situations when the transmission is overloaded.

In the Figure 7 shown a calculated approximation (with the norm in a least squares sense) with the velocity v from 0.12 m/s (the measured values of friction with a relatively small velocity can be disturbed by the elasticity of the belt), by linear function:

$$\mu(v) = c_{1v} \cdot v + c_{2v}, \quad (4)$$

where:

v – tangential velocity in contact,

c_{1v} , c_{2v} – coefficients to calculate for each case of preload force F_0 .

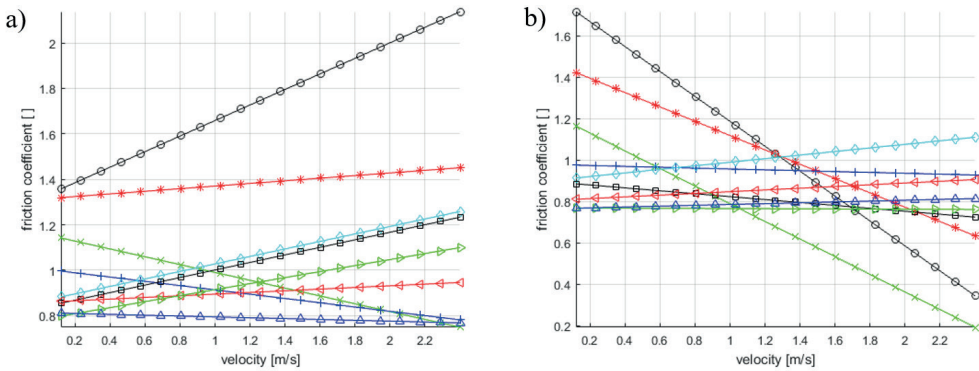


Fig. 7. Linear approximation of values of effective dynamic friction coefficient as a function of velocity, for wrap angle: a) $\alpha = 45^\circ$, b) $\alpha = 90^\circ$

$\circ F_0=200$ N, $* F_0=300$ N, $\times F_0=400$ N, $+ F_0=500$ N, $\diamond F_0=600$ N, $\square F_0=700$ N, $\triangle F_0=800$ N, $\nabla F_0=900$ N, $\triangle F_0=1000$ N

In Table 1, calculated coefficients of the function of the assumed approximation are shown.

Tab. 1. Calculated coefficient of the first approximation

| Wrap angle $\alpha = 45^\circ$ | | | | Wrap angle $\alpha = 90^\circ$ | | | |
|--------------------------------|----------|----------|-------|--------------------------------|----------|----------|-------|
| F_0 | c_{1v} | c_{2v} | Norm | F_0 | c_{1v} | c_{2v} | Norm |
| 200 N | 0.342 | 1.316 | 4.336 | 200 N | -0.602 | 1.789 | 4.188 |
| 300 N | 0.058 | 1.313 | 3.871 | 300 N | -0.346 | 1.464 | 3.896 |
| 400 N | -0.173 | 1.162 | 2.804 | 400 N | -0.426 | 1.215 | 2.168 |
| 500 N | -0.094 | 1.007 | 2.234 | 500 N | -0.021 | 0.978 | 2.314 |
| 600 N | 0.165 | 0.862 | 1.729 | 600 N | 0.086 | 0.903 | 1.470 |
| 700 N | 0.166 | 0.835 | 1.915 | 700 N | -0.071 | 0.894 | 1.571 |
| 800 N | 0.037 | 0.858 | 1.262 | 800 N | 0.042 | 0.805 | 1.522 |
| 900 N | 0.132 | 0.782 | 1.567 | 900 N | -0.003 | 0.768 | 1.132 |
| 1000 N | -0.019 | 0.813 | 1.292 | 1000 N | 0.021 | 0.765 | 1.024 |

First, what can be noticed from the figures is a difficulty in finding one general friction dependence on the relative velocity. Some of them increase, some decrease and different slopes occur. It was, therefore, decided to calculate some average values. The calculated values are a function of the preload force shown in the Figure 8. Figure 8a corresponds with wrap angle $\alpha = 45^\circ$, whereas Figure 8b corresponds with wrap angle $\alpha = 90^\circ$.

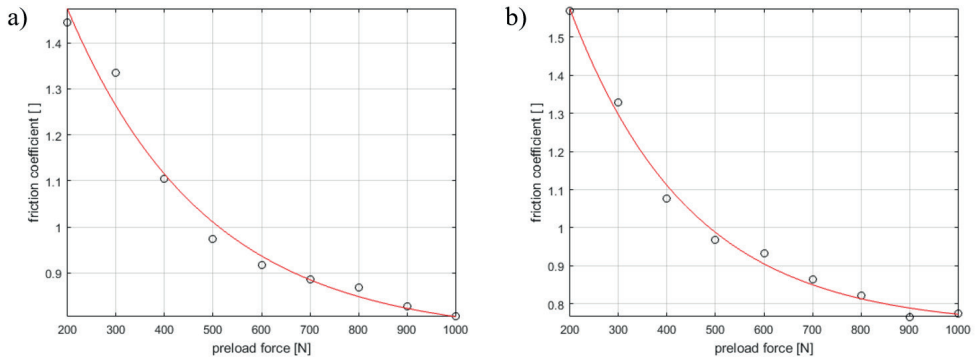


Fig. 8. Approximation of the average values of effective dynamic friction as a function of preload force F_0 , for wrap angle: a) $\alpha = 45^\circ$, b) $\alpha = 90^\circ$

In the figures (8), the results of the approximation are also shown. The approximation function was assumed as:

$$\mu(F_0) = e^{-c_{1F_0}(F_0 - c_{2F_0})} + c_{3F_0}, \quad (5)$$

where:

c_{1F_0} , c_{2F_0} , c_{3F_0} – coefficients to calculate.

Coefficient c_{1F_0} influences the shape of the curve, whereas coefficients c_{2F_0} and c_{3F_0} translate the curve along the x axis and the y axis, respectively.

The values of the unknown coefficients were determined using the Nelder-Mead nonlinear optimisation method by comparing the resulting curves with results obtained experimentally. The norm as an objective function was assumed as follows:

$$F_{fit} = \sqrt{\sum_{i=1}^n (\mu(F_0) - \mu_e(F_0))^2}, \quad (6)$$

where:

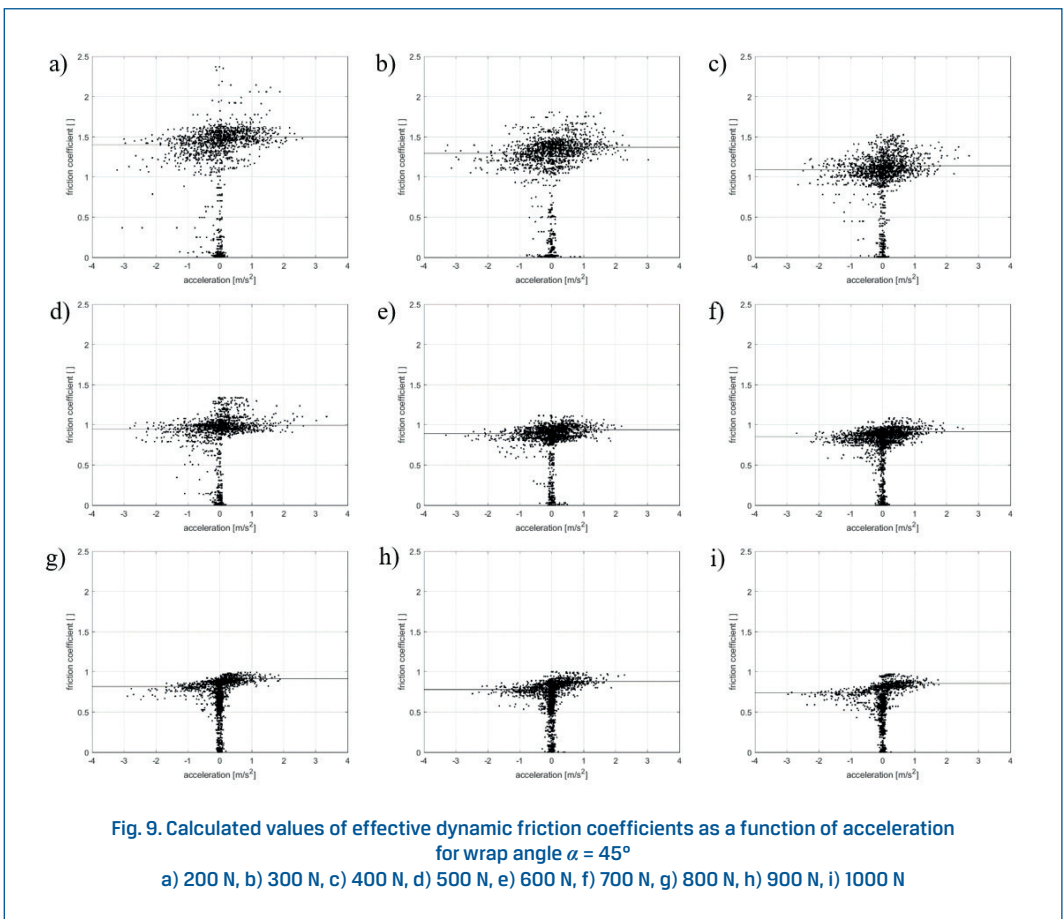
$\mu_e(F_0)$ – values of the friction coefficient achieved during the experiments.

In Table 2 shown the calculated values of the approximation coefficients.

Tab. 2. Calculated coefficients of the second approximation

| Wrap angle | c_1F_0 | c_2F_0 | c_3F_0 | Norm |
|---------------------|----------|----------|----------|--------|
| $\alpha = 45^\circ$ | 0.0035 | 103.5686 | 0.7619 | 0.0913 |
| $\alpha = 90^\circ$ | 0.0041 | 155.1994 | 0.7405 | 0.0645 |

Next, in the Figure 9 and Figure 10, the calculated values of the friction coefficient are presented as a function of translational acceleration in joint for wrap angles $\alpha = 45^\circ$ and 90° , respectively. As can be noticed from the figures, it is much easier to see some predictability than in those presenting coefficient values as a function of the velocity. Of course, when the preload force is greater, the results are more and more consistent.



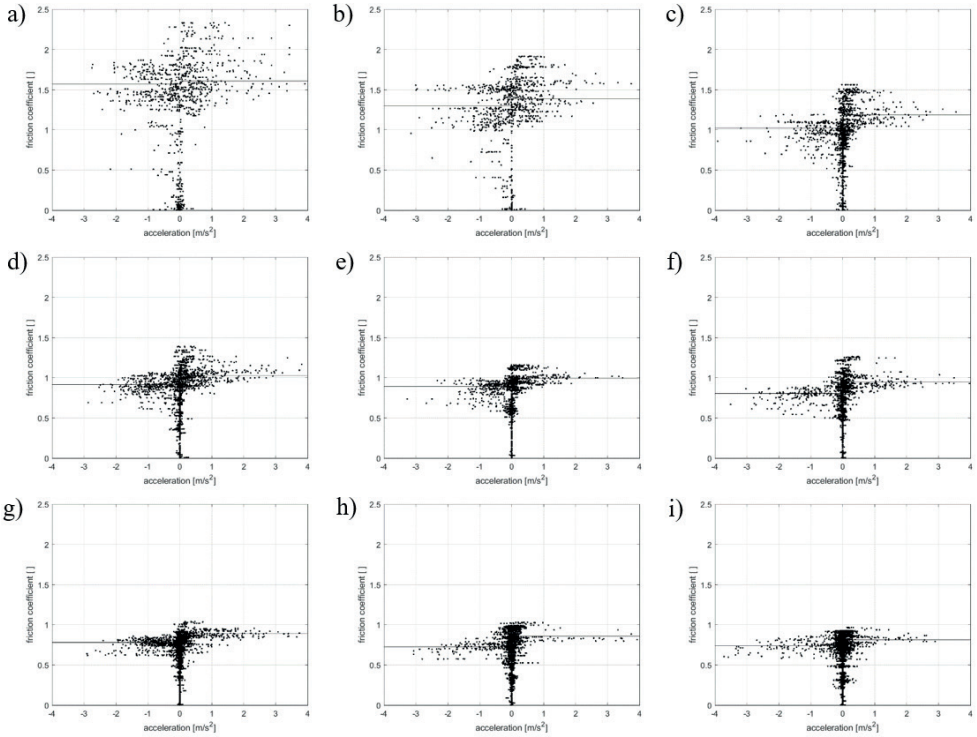


**Fig. 10. Calculated values of effective dynamic friction coefficients as a function of acceleration for wrap angle $\alpha = 90^\circ$
a) 200 N, b) 300 N, c) 400 N, d) 500 N, e) 600 N, f) 700 N, g) 800 N, h) 900 N, i) 1000 N**

As can be seen, in some cases of friction preload, the values of the friction coefficient differ slightly for negative and positive values of acceleration, but for increasing absolute values of acceleration, they appear to be constant. For negative values of acceleration, the values of the calculated friction coefficient seem to be less than the values for positive acceleration. It is partly caused by the inertia of the belt and the pulley and changing conditions between increasing and decreasing velocity.

It was proposed to approximate the friction coefficient as a function of acceleration using the following function:

$$\mu(a) = \begin{cases} c_{1a} & \text{for } a \leq -a_{\max} \\ c_{1a} + (c_{2a} - c_{1a}) \cdot d^2 \cdot (3 - 2d) & \text{for } -a_{\max} < a < a_{\max} \\ c_{2a} & \text{for } a \geq a_{\max} \end{cases} \quad (7)$$

where:

$$d = \frac{a + a_{\max}}{2a_{\max}}$$

$a_{\max} = 0.5 \frac{\text{m}}{\text{s}^2}$ – arbitrary value of acceleration defining the boundary value of sticking,
 a – tangential acceleration in contact,
 c_{1a} c_{2a} – coefficients to be calculated for each case of preload force F_0 .

The shape of the function presented above is shown schematically in the Figure 11.

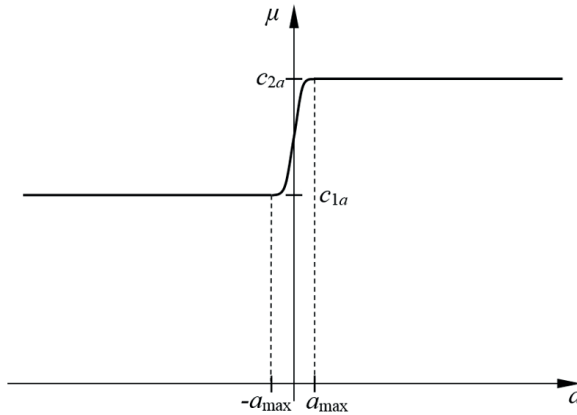


Fig. 11. Assumed approximation function

As it was assumed during earlier approximation, during the present approximation process, the values of friction with acceleration near zero (assumed as $-0.4 < a < 0.4$) were not analysed and it also assumed a similar norm. It is worth mentioning that despite the assumed value of ignored acceleration, there is no reason to assume the same value as the previously mentioned parameter a_{\max} . It should rather be selected from literature or through a verification of the particular model of friction with experiments.

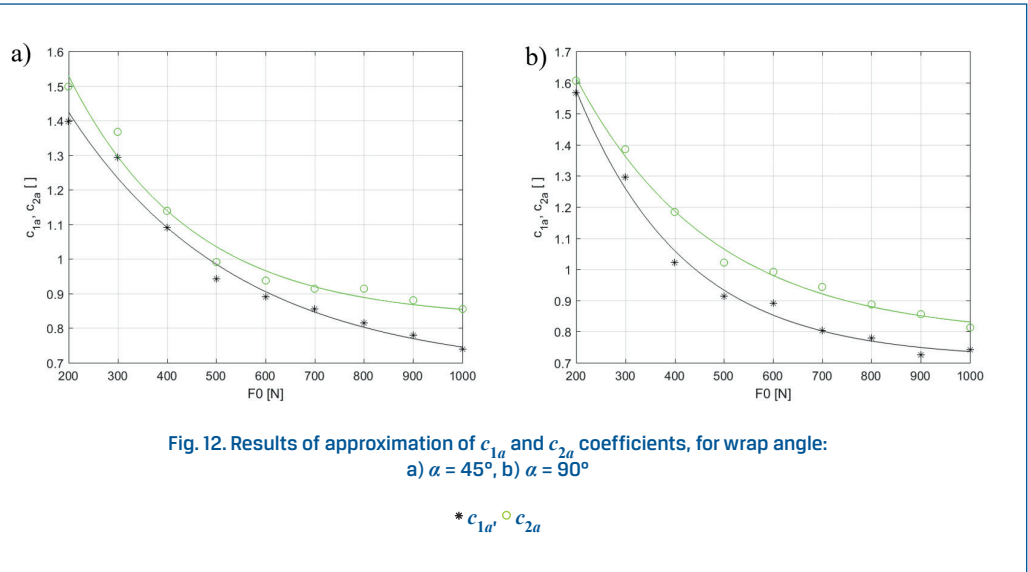
The resulting approximation lines are also shown in the Figure 9 and Figure 10.

In Table 3 shown the calculated coefficients of the calculated approximation function. What is especially interesting is that, generally, the norm decreases with an increasing normal force.

Tab. 3. Calculated coefficients of the third approximation

| Wrap angle $\alpha = 45^\circ$ | | | | Wrap angle $\alpha = 90^\circ$ | | | |
|--------------------------------|----------|----------|--------|--------------------------------|----------|----------|--------|
| F_0 | c_{1a} | c_{2a} | Norm | F_0 | c_{1a} | c_{2a} | Norm |
| 200 N | 1.3976 | 1.4980 | 3.0876 | 200 N | 1.5666 | 1.6062 | 4.0497 |
| 300 N | 1.2930 | 1.3671 | 2.8672 | 300 N | 1.2955 | 1.3863 | 3.5237 |
| 400 N | 1.0910 | 1.1397 | 2.1413 | 400 N | 1.0219 | 1.1844 | 1.7158 |
| 500 N | 0.9428 | 0.9915 | 1.7043 | 500 N | 0.9138 | 1.0224 | 1.7750 |
| 600 N | 0.8903 | 0.9372 | 1.2748 | 600 N | 0.8908 | 0.9917 | 1.0563 |
| 700 N | 0.8546 | 0.9136 | 1.3595 | 700 N | 0.8034 | 0.9443 | 1.0642 |
| 800 N | 0.8156 | 0.9136 | 0.6217 | 800 N | 0.7789 | 0.8875 | 0.8705 |
| 900 N | 0.7794 | 0.8799 | 0.9044 | 900 N | 0.7254 | 0.8563 | 0.7333 |
| 1000 N | 0.7392 | 0.8556 | 0.6010 | 1000 N | 0.7412 | 0.8126 | 0.7935 |

All results combined are presented in the Fig.12.



What is especially interesting is that all coefficients decrease when the preload force simultaneously increases. But it must be noticed that, in all cases, the dependences are not linear.

It was, therefore, decided to conduct the approximation process again for the presented results. The approximation functions were assumed as:

$$c_{1a}(F_0) = e^{-c_{11a}(F_0 - c_{12a})} + c_{13a}, \tag{8a}$$

$$c_{2a}(F_0) = e^{-c_{21a}(F_0 - c_{22a})} + c_{23a}. \tag{8b}$$

The following values were calculated during the approximation process:

- for wrap angle $\alpha = 45^\circ$:

$$c_{11a} = 0.0029, \quad c_{12a} = 102.4917, \quad c_{13a} = 0.6735 \quad (\text{with calculated norm } 0.0815),$$

$$c_{21a} = 0.0040, \quad c_{22a} = 112.6208, \quad c_{23a} = 0.8061 \quad (\text{with calculated norm } 0.0983),$$

- for wrap angle $\alpha = 90^\circ$:

$$c_{11a} = 0.0045, \quad c_{12a} = 167.2391, \quad c_{13a} = 0.7132 \quad (\text{with calculated norm } 0.0727),$$

$$c_{21a} = 0.0036, \quad c_{22a} = 148.0357, \quad c_{23a} = 0.7845 \quad (\text{with calculated norm } 0.0598).$$

3. The model of the transmission

The model applied the achieved values of friction to a two-dimensional model of a belt transmission presented, among others, in [9].

In the Figure 13 schematically shown the assumed transmission, which consists of four pulleys of the same radius of $r=0.19$ m. The origins of the pulleys are as follows: $O_1=(0,0)$, $O_2=(0,-1)$, $O_3=(1,-1)$, $O_4=(1,0)$. This is applied to the driving torque of the first pulley. Resistance torque is also applied to only one (fourth) pulley. The rest of the pulleys rotate without any resistance in their bearings. The initial preload force of the belt is assumed as $F_0 = 500$ N, which causes a relatively large rolling resistance. The wrap angles in every pulley equal 90° in the case of each pulley. The same wrap angle was considered in one of the configurations of the research stand.

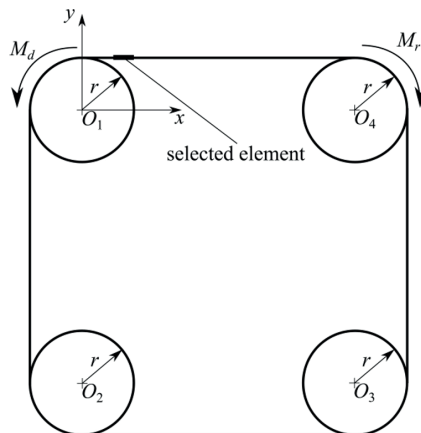


Fig. 13. The transmission assumed

The friction force has been implemented based on earlier measurements (especially from formula 8) and assumed as a function of acceleration, preload force F_0 and normal force N between the belt element and the pulley:

$$F_F = \delta(v)\mu(a, F_0)N, \quad (9)$$

where:

$\delta(v)$ – coefficient described by a similar formula as (7):

$$\delta(v) = \begin{cases} -1 & \text{for } v \leq -\Delta v \\ -1 + 2d'^2 \cdot (3 - 2d') & \text{for } -\Delta v < v < \Delta v \\ 1 & \text{for } v \geq \Delta v \end{cases} \quad (10)$$

where:

$$d' = \frac{v + \Delta v}{2\Delta v},$$

The course of parameter $\delta(v)$ shown in the Figure 14. Parameter Δv is assumed as 10^{-3} m/s.

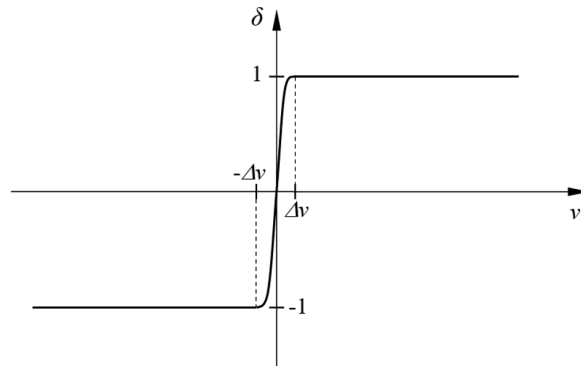


Fig. 14. Course of the assumed coefficient $\delta(v)$

Translational and rotational stiffness and damping coefficients are assumed based on related own works and [2, 3, 4]. The contact model is assumed from a previous own article [9].

In the Figure 15 shown the courses of the torques applied to the pulleys. As can be see, the driving pulley rotates with a constant torque of $M_d=15$ Nm. Positive values of the driving torque cause anti-clockwise rotations of the pulleys.

Resistance torque M_r , is also applied, with an increasing value from 0 Nm to 15 Nm in 2 s (and opposite direction of the vector in relation to the driving pulley). After this moment, the value remains constant.

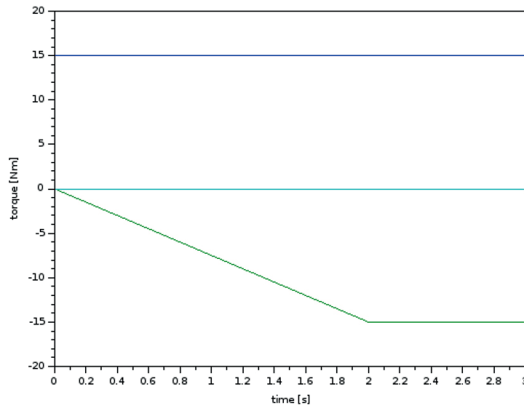


Fig. 15. Courses of torques applied to:

— 1st pulley, — 2nd pulley, — 3rd and 4th pulley

In the Figure 16 presented the achieved courses of angular velocities of the chosen two pulleys: driving and driven. As can be seen, in general, the calculated velocities are similar. Slight differences between courses result from belt slip. The bifurcations of courses are resulting from belt vibrations and of the assumed discrete model of the belt (normal and friction forces are calculated individually, which influences the entire system). Achieved fluctuations after 2 s resulting from oscillating mass of driven pulley.

The assumed driving torque is relatively large, and it should make for a relatively rapid start of the transmission. But, the applied resistance torque and rolling resistance torque causes that, after 2 s, the transmission stops almost immediately. It was registered that the maximum value of the angular velocity achieved 28 rad/s in about 0.55 s.

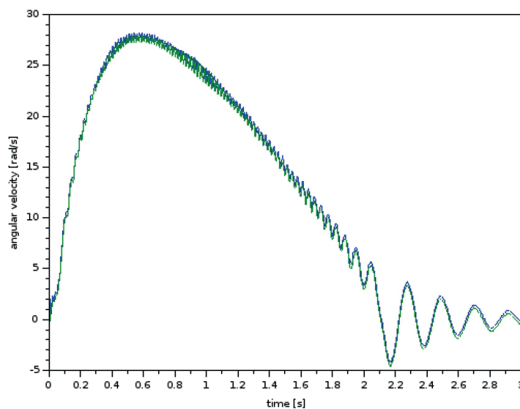


Fig. 16. Calculated courses of angular velocities

— driving (1st) pulley, — driven (4th) pulley

In the Figure 17 presented the calculated courses of reaction forces in the longitudinal spring-damping element connecting the chosen beam element (specified in the Figure 13) and the neighbouring (right side) beam element. In periods of (0.0-0.2) s and (1.05-1.3) s, the chosen spring-damping element was in the active (upper) part of the belt, which causes higher values of reaction force. After the transmission has stopped, the force stabilised at a value of about 475 N. The element was in one of the passive (bottom) parts of the belt.

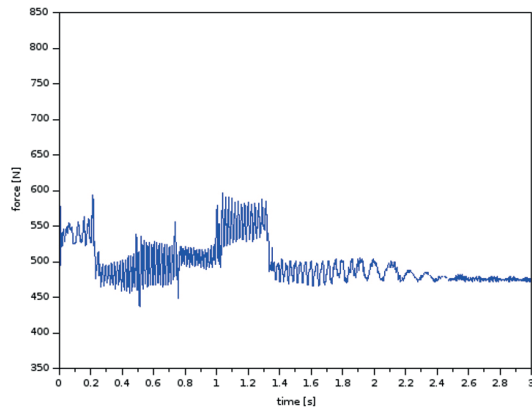


Fig. 17. Calculated course of the reaction force in a selected longitudinal spring-damping element

The selected belt element starts just before the 1st pulley. In the Figure 18 shown the courses of the normal force (Figure 18a) and the friction force (Figure 18b) between the chosen element and the pulleys. Nonzero values of forces appear during contact with pulleys, respectively: 1st, 2nd, 3rd, 4th, 1st, 2nd. The chosen element stops after 2 s between the 2nd and the 3rd pulley.

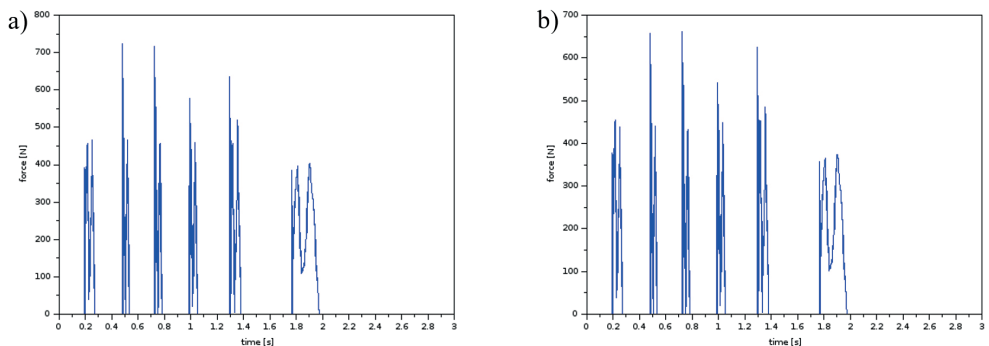


Fig. 18. Calculated courses of: a) normal force, b) friction force

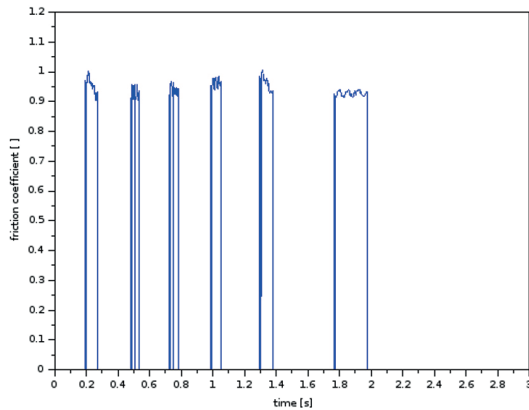


Fig. 19. Calculated course of the effective friction coefficient

In the Figure 19 shown the calculated values of the effective friction coefficient. As can be see, the values were oscillating between approx. 0.9 and 1. During the contact of the belt element with the pulleys, the value of the friction coefficient continuously changes. When the belt element starts to contact the driving pulley, the acceleration increases immediately and then changes its value to negative when it leaves the pulley. As concluded in the previous chapter, the value of the friction coefficient for positive values of acceleration is greater than that measured for negative values. This is the reason why the value of the friction coefficient decreases during contact with the driving pulley, which is clearly visible in the figure.

The situation is different when it contacts the pulley with resistance torque applied. The acceleration of the belt element increases (the value of the friction coefficient increases too).

It is not possible to unambiguously identify the value of the friction coefficient in contact with a loose pulley. Most often, the acceleration will oscillate in values close to zero.

4. Conclusions

The presented results prove that the value of the effective friction coefficient depends on the relative translational velocity between the belt and the pulley, but this assumption is not enough. What is especially interesting is that the values can differ for positive and negative values of acceleration. This means that its values are different when the velocity increases or decreases.

Next, what was discovered when the standard Euler-Eytelwein formula was assumed was that the coefficient decreases with increasing belt tension. To ensure that this is the correct conclusion, two cases of wrap angles were measured. It proves how important it is to

design a proper preload force in the transmission. It should be selected from manufacturers guidelines. Too much tension can cause a worse efficiency of the transmission.

It is obvious that the results of the measurements would be more precise if the values of belt elasticity were known. But, it is worth mentioning that the measured group of poly-V belts are relatively rigid because of their relatively small height-to-width proportion.

The measured results and conclusions can, of course, depend on the belt measured, because they can differ in chemical and physical properties of the working surfaces. A measurement group of belts from different manufacturers should constitute a further objectives of research. It is also planned to measure friction forces of the belt-pulley pair with some impurities.

5. References

- [1] Bechtel S.E., Vohra S., Jacob K.I., Carlson C.D.: The stretching and slipping of belts and fibers on pulleys, *Journal of Applied Mechanics*, 67, 2000, 197-206, DOI: 10.1115/1.321164
- [2] Čepon G., Boltežar M.: Dynamics of a belt-drive system using a linear complementarity problem for the belt-pulley contact description, *Journal of Sound and Vibration*, 319, 2009, 1019-1035, DOI: 10.1016/j.jsv.2008.07.005
- [3] Čepon G., Manin L., Boltežar M.: Experimental identification of the contact parameters between a V-ribbed belt and a pulley, *Mechanism and Machine Theory*, 45, 2010, 1424-1433, DOI: 10.1016/j.mechmachtheory.2010.05.006
- [4] Čepon G., Manin L., Boltežar M.: Introduction of damping into the flexible multibody belt-drive model: A numerical and experimental investigation, *Journal of Sound and Vibration*, 324, 2009, 283-296, DOI: 10.1016/j.jsv.2009.02.001
- [5] Chen G.(S.), Lee J.H., Narravula V., Kitchin T.: Friction and noise of rubber belt in low temperature condition. The influence of interfacial ice film, *Cold Regions Science and Technology*, 71, 2012, 95-101, DOI: 10.1016/j.coldregions.2011.10.007
- [6] Cruz Gómez M.A., Gallardo-Hernández E.A., Vite Torres M., Peña Bautista A.: Rubber steel friction in contaminated contacts, *Wear*, 302, 2013, 1421-1425, DOI: 10.1016/j.wear.2013.01.087
- [7] Fawcett J.N.: Chain and belt drives – a review, *Shock Vibrations Digest*, 13(5), 1981, 5-12, DOI: 10.1177/058310248101300503
- [8] Kim D., Leamy M.J., Ferri A.A.: Dynamic Modeling and Stability Analysis of Flat Belt Drives Using an Elastic/Perfectly Plastic Friction Law, *ASME Journal of Dynamic Systems, Measurement, and Control*, 133, 2011,1-10, DOI: 10.1115/1.4003796
- [9] Kubas K.: A model for the dynamic analysis of a belt transmission using the Dahl friction model, *Journal of Theoretical and Applied Mechanics*, 55, 4, 2017, 1423-1435, DOI: 10.15632/jtam-pl.55.4.1423
- [10] Leamy M.J., Wasfy T.M.: Analysis of belt-drive mechanics using a creep-rate-dependent friction law, *Journal of Applied Mechanics*, *Transactions of the American Society of Mechanical Engineers*, 69, 6, 2002, 763-771, DOI: 10.1115/1.1488663.
- [11] Leamy M.J., Wasfy T.M.: Transient and Steady-State Dynamic Finite Element Modeling of Belt-Drives, *ASME Journal of Dynamic Systems, Measurement, and Control*, 124, 4, 2002, 575-581, DOI: 10.1115/1.1513793.
- [12] Li K.W., Chen C.J. The effect of shoe soling thread groove width on the coefficient of friction with different sole materials, floors, and contaminants, *Applied Ergonomics*, 35, 2004, 499-507, DOI: 10.1016/j.apergo.2004.06.010
- [13] Manin L., Lorenzon C., Saad H.: Belt-pulley friction coefficient, experimental analysis: Influence of the Poly-V belt material components and contact pressure, *Proceedings of the International Conference on Power Transmissions*, Chongqing, China, 2016, DOI: 10.1201/9781315386829-9
- [14] Manin L., Liang X., Lorenzon C.: Power losses prediction in poly-v belt transmissions: application to front

engine accessory drives, Proceedings of International Gear Conference, Lyon, France, 2014, 1162-1171, DOI: 10.1533/9781782421955.1162

- [15] Mofidi M., Kassfeldt E., Prakash B.: Tribological behaviour of an elastomer aged in different oils, Tribology International, 41, 2008, 860-866, DOI: 10.1016/j.triboint.2007.11.013
- [16] Sheng G., Lee J.H., Narravula V., Song D.: Experimental characterization and analysis of wet belt friction and the vibro-acoustic behavior, Tribology International, 44, 2011, 258-265, DOI: 10.1016/j.triboint.2010.10.025